Alignment and nonlinear elasticity in biopolymer gels

Jingchen Feng,[1] Herbert Levine,[1] Xiaoming Mao,[2] and Leonard M. Sander[3]
[1]*Bioengineering Department and Center for Theoretical Biological Physics, Rice University, Houston, Texas 77251-1892, USA*
[2]*Department of Physics, University of Michigan, Ann Arbor, Michigan 48109-1040, USA*
[3]*Physics & Complex Systems, University of Michigan, Ann Arbor, Michigan 48109-1040, USA*
(Received 3 June 2014; revised manuscript received 2 October 2014; published 15 April 2015)

We present a Landau-type theory for the nonlinear elasticity of biopolymer gels with a part of the order parameter describing induced nematic order of fibers in the gel. We attribute the nonlinear elastic behavior of these materials to fiber alignment induced by strain. We suggest an application to contact guidance of cell motility in tissue. We compare our theory to simulation of a disordered lattice model for biopolymers. We treat homogeneous deformations such as simple shear, hydrostatic expansion, and simple extension, and obtain good agreement between theory and simulation. We also consider a localized perturbation which is a simple model for a contracting cell in a medium.

DOI: 10.1103/PhysRevE.91.042710 PACS number(s): 87.10.Pq, 82.35.Pq, 62.20.D−, 87.17.Jj

I. INTRODUCTION

Biopolymer gels are complicated materials consisting of a network of cross-linked polymer chains. Almost all of these materials show nonlinear elasticity, usually strain stiffening. Typically, the shear modulus increases by an order of magnitude under applied strain [1–3]. These materials are important in biology; for example, in the body there is almost always a gel, the extracellular matrix (ECM) which gives tissue its structure. The biopolymer Collagen-I is the most common constituent of the ECM. When cells migrate within tissue—for example, in wound healing and cancer invasion—they crawl by attaching to the gel fibers [4]. When cells move in this fashion they deform the ECM. However, deformation also affects cell motility. In particular, if the fibers in the ECM are partially aligned, cells tend to move along the aligned direction—this is called *contact guidance* [5,6]. Since cells deform and align the ECM, and their motility is affected by this deformation, mechanically mediated *cell-cell interactions* are to be expected [4,6]. In this paper we formulate a theory for the nonlinear elasticity in biopolymers to give a framework for understanding moving cells.

We concentrate on a model for Collagen-I. We note that it is an athermal biopolymer: i.e., the elasticity of the individual fibers is purely mechanical because the thermal correlation length is far larger than the mesh size [7]. The model we present is specialized to this case. Further, the strain on individual fibers is modest so that the nonlinear strain stiffening of the matrix arises from linear elements [7,8] in contrast to other biopolymers [3]. For small strains the elasticity is dominated by the (small) bending modulus of the fibers—different parts of the disordered material turn with respect to one another so that the deformation is nonaffine because there are soft bending modes. As strains increase, bending modes are "exhausted" and for large strains the material is aligned, and must stretch (Fig. 1). The large stretching modulus then determines the response and the deformation is affine. A plausible order parameter to describe the transition is precisely the *alignment of the fibers*: it is a measure of the exhaustion of the soft modes. The claim is that the nonlinear elasticity of Collagen-I is usefully connected to the "hidden" variable, alignment.

To quantify alignment we use the nematic order parameter, familiar from the study of liquid crystals. Collagen-I does not have a nematic instability, but it can be aligned by stress to give a nonzero value of the nematic tensor, $\mathbf{Q}$, describing the local directions of the polymers,

$$\mathbf{Q}(\mathbf{r}) \equiv \left\langle \hat{v}\hat{v} - \frac{1}{d} I \right\rangle. \tag{1}$$

Here $\hat{v}$ is the unit vector pointing along the orientation of the polymers within the volume element at $\mathbf{r}$, and the average $\langle \cdots \rangle$ is over all fibers within the volume element, weighted by the fiber length. This volume element, which is the scale that our theory applies to, is much greater than the mesh size of the network, but much smaller than macroscopic length scale. As a result, in the undeformed state, $\mathbf{Q} = 0$ because local anisotropy is averaged out. In what follows we will use a scalar, q, $0 \leqslant q \leqslant 1$, to characterize the strength of the alignment. We define $q = [d/(d-1)]\lambda_m$, where λ_m is the largest eigenvalue of $\mathbf{Q}$. In two dimensions, $q = \langle \cos(2\theta) \rangle$, where θ is the direction of the polymer chain measured from the aligned direction. This measure was used in the experiments of Ref. [6].

We proceed by formulating a Landau theory for biopolymers along the lines suggested in Ref. [9] for nematic elastomers. We use two coupled order parameters, the strain tensor and $\mathbf{Q}$. We test the framework by fitting our theory to a disordered lattice model which share many feature with Collagen-I [10–13]. The unique feature of our approach is that all of the Landau coefficients are determined explicitly, allowing a detailed test of the modeling. Then we insert a "cell," i.e., a localized source of deformation, to begin to address the questions above.

II. FORMULATING A LANDAU-TYPE THEORY

A. Shear deformation

First, we model the nonlinear elastic energy under shear deformation only. Volume-changing deformations will be treated later. The energy is a functional of the deformation gradient tensor [9]: $\Lambda_{ij} = \partial R_i/\partial r_j = \delta_{ij} + \partial_j u_i$. Here $\mathbf{r}$ is a point in the reference space, $\mathbf{R}$ is its image in the deformed space, and i, j are Cartesian indices. From this we form the

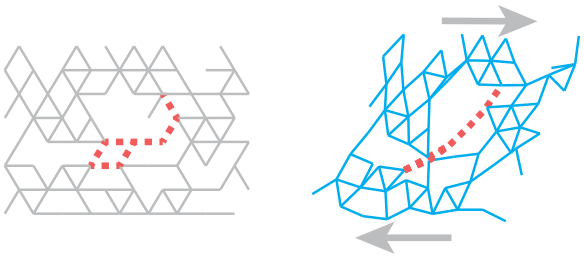

FIG. 1. (Color online) Small area of a network before (left) and after (right) simple shear. Red dashed lines: the part of the fiber segments that align with the direction of strain after easy bending modes are exhausted. Solid lines: other fiber segments before (gray) and after (blue) deformation.

left Cauchy-Green strain tensor:

$$\mathbf{v} = (1/2)(\Lambda\Lambda^T - \mathbb{I}). \tag{2}$$

The volume element in the deformed space is $\det(\Lambda) \to 1 + \mathrm{Tr}\,\mathbf{v}$, where the last form is for the linear regime.

For the moment we consider simple shear so that, to lowest order, we need the traceless part of $\mathbf{v}$ which we call $\tilde{\mathbf{v}}$. We propose the following free energy:

$$F_s = \int [\bar{\mu}\,\mathrm{Tr}\,\tilde{\mathbf{v}}^2 - t\,\mathrm{Tr}(\tilde{\mathbf{v}}\cdot\mathbf{Q}) + V(\mathbf{Q})]d^dr, \tag{3}$$

where $\bar{\mu}$ is the shear modulus. The bar on $\bar{\mu}$ means that it is a "bare" value. The observed shear modulus, μ, is gotten by renormalizing $\bar{\mu}$ by coupling to $\mathbf{Q}$, as we will see. The potential for the nematic order, $V(\mathbf{Q})$, is the energy cost to align the network against the constraints.

The term $-t\,\mathrm{Tr}(\tilde{\mathbf{v}}\cdot\mathbf{Q})$ is the leading-order coupling between strain and alignment allowed by symmetry. The order parameter, $\mathbf{Q}$, which describes the alignment induced by strain, transforms as a tensor in the deformed state so that it has the same symmetry as $\tilde{\mathbf{v}}$. Their contraction is a scalar that can enter the free energy. Because $\mathbf{Q}$ is traceless, in leading order the alignment responds to shear and not to hydrostatic deformations. This form of coupling between strain and local material anisotropy is similar to Cosserat (micropolar) elasticity [14,15].

The auxiliary variable $\mathbf{Q}$ is not necessary in our formulation. We could, in traditional fashion, write an explicitly nonlinear theory instead of Eq. (3)—it would correspond to our model after "integrating out" $\mathbf{Q}$. We do not do this for several reasons: first, $\mathbf{Q}$ is observable [6] and gives useful information about the system. Also, if we formulate the model in terms of $\mathbf{Q}$ it is rather simple and physically motivated. There is no obvious way to pick the nonlinear terms in a traditional formulation, but they arise naturally in our method. Finally, this theory gives a good way to deal with contact guidance.

For small deformations, linear elasticity, we keep the leading-order term for the potential, $V \approx (A/2)\mathrm{Tr}\mathbf{Q}^2$. Minimizing F for fixed $\mathbf{v}$ gives $\mathbf{Q} = (t/A)\tilde{\mathbf{v}}$. Thus *strain induced alignment* is a linear response for small deformations. Since this relation is determined by symmetry, we expect it to hold for all biopolymer gels. Now $\mathbf{Q}$ can be eliminated from F, recovering linear elasticity:

$$F \to \int [\mu\,\mathrm{Tr}\tilde{\mathbf{v}}^2]d^dr, \quad \mu = \bar{\mu} - t^2/2A, \tag{4}$$

with an effective shear modulus, $\mu < \bar{\mu}$.

At larger deformations, nonlinear terms in V start to dominate and $\mathbf{Q}$ falls below the linear response value. The effective shear modulus increases from its value in the linear regime, giving strain stiffening. In the extreme case of $\mathbf{Q}$ reaching a saturated value $\mathbf{Q}_{\max}$ independent of $\mathbf{v}$, we get $\bar{\mu} \simeq \mu$.

The nonlinearity in $V(\mathbf{Q})$ can be interpreted. At small strain the deformation in a dilute network consists mostly of nonaffine deformations involving bending of fibers. At greater strain, the deformation crosses over into deformation involving stretching of fibers, because the easy bending modes become exhausted, as shown in Fig. 1. As a result, the increase of $\mathbf{Q}$ will eventually saturate. In contrast, for denser networks, there are fewer weak modes, even for small deformations the system is mostly affine, stretching dominated, and the alignment follows the geometry of the deformation. As a result, the crossover disappears, and the network has a more linear increase of $\mathbf{Q}$ as strain increases. We thus expect the nonlinearity in $V(\mathbf{Q})$ to be strong for dilute networks and weak for dense ones. This is verified in simulations; see below.

B. Volume-changing deformation

Now we consider volume-changing deformations such as hydrostatic expansion. There is a conceptual difficulty here since, for this case, there is no average alignment. Nevertheless, there can be nonlinearity in the bulk modulus. For example, the filamentous triangular lattice model [10–13] (discussed in more detail below) shows similar strain-stiffening effects in bulk and shear moduli (Fig. 2). Such strain stiffening in hydrostatic expansion has been studied in Ref. [16] via simulation and in effective medium theory. To capture this effect in our Landau-type theory, we note that even for hydrostatic expansion, there will be *local* alignment and weak parts of the disordered system will rotate and the deformation is nonaffine. It is worth pointing out that similar to the averaging volume element of our definition of $\mathbf{Q}$, such local alignment occurs at a scale much greater than the mesh size. Thus a local nonzero $\mathbf{Q}$ only emerges with the deformation, and $\mathbf{Q} = 0$ in the undeformed state. The emergent alignment at such scale is clear in the simulation. At large strain, deformations cross over to affine, stretching dominant, similar to the case of shear.

We treat such effects of disorder by introducing a random tensor field, $\mathbf{h}(\mathbf{r})$ with $\langle\mathbf{h}\rangle = 0, \langle\mathbf{h}(\mathbf{r})\cdot\mathbf{h}(\mathbf{s})\rangle = g\delta(\mathbf{r}-\mathbf{s})\mathbb{I}$, which accounts for disorder effects on the alignment field. Using $\mathbf{h}$ we can form a scalar, $\mathrm{Tr}(\mathbf{h}\cdot\mathbf{Q})$, which can couple to volume change. To characterize the volume change we introduce $Y = 2(\sqrt{\det\Lambda} - 1) \to \mathrm{Tr}\mathbf{v}$. The last form is in the linear regime. We have specialized to two dimensions so that we can compare to a two-dimensional model below. This form of volume change is proportional to the extension of the fibers in the network. The elastic energy for affine deformations is strictly quadratic in Y. Now we add to Eq. (3) the following

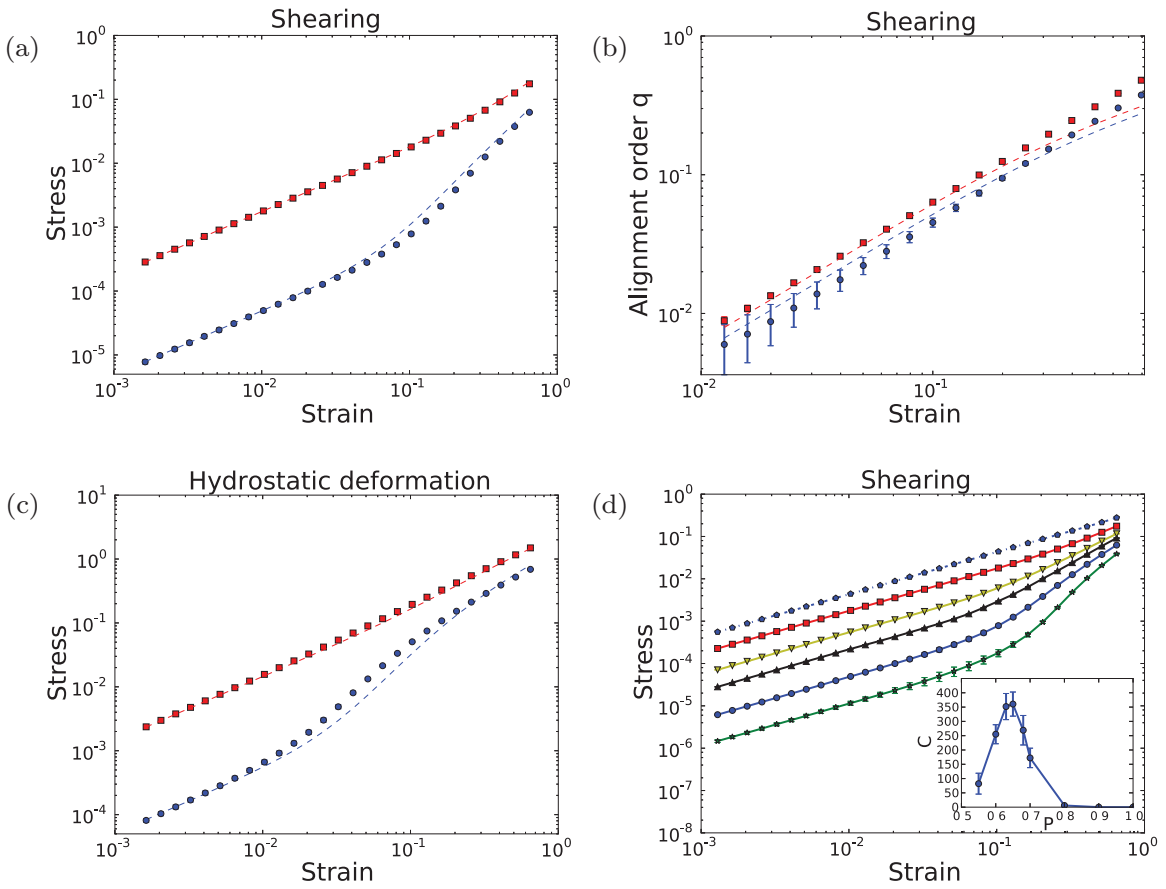

FIG. 2. (Color online) (a) Simulation (data points) and model fit (dashed curves) based on Eqs. (3) and (5) for shear stress as a function of strain, for lattices with $p = 0.6$ (lower blue), and $p = 0.8$ (higher red). (b) Alignment order q as function of shear strain for the same deformation and color coding as in (a). (c) Stress as a function of strain for hydrostatic deformations for lattices with $p = 0.6$ (lower blue), and $p = 0.8$ (higher red). (d) Stress strain curves for shear deformation at more values of p (from top to bottom, $p = 1.00, 0.80, 0.70, 0.65, 0.60, 0.55$). Inset: fitted parameter $C(p)$, which controls the nonlinearity in V. For (a)–(d) we used $\kappa/(ka^2) = 10^{-3}$.

terms:

$$F_h = \int \left[\frac{1}{2}\bar{K}Y^2 - Y\,\mathrm{Tr}(\mathbf{h}\cdot\mathbf{Q})\right] d^d r. \tag{5}$$

The coupling term between Y and $\mathrm{Tr}(\mathbf{h}\cdot\mathbf{Q})$ is the leading-order term that controls the nonlinearity in the bulk modulus. [There is no term of the form $\mathrm{Tr}(\mathbf{h}\cdot\mathbf{v})$ because it would give a net stress on the lattice in the reference state.] The total energy is $F_s + F_h$. Once more, we have a bare quantity, $\bar{K}$, the bare bulk modulus.

We follow the steps above to see how renormalization of the bulk modulus occurs. For a hydrostatic expansion, we minimize F with respect to $\mathbf{Q}$ and find, in the linear regime, $\mathbf{Q} = (\mathrm{Tr}\mathbf{v}/A)\mathbf{h}$, a linear response. Putting this form back into F and taking the disorder average gives, as in the case of $\bar{\mu}$, $K = \bar{K} - 2g/A$. For large strain the renormalization is smaller, and $K \to \bar{K}$, as above.

III. CALIBRATING THEORY WITH NUMERICAL SIMULATION

To calibrate Eqs. (3) and (5) we apply the theory to a model for biopolymer gels based on a triangular lattice of lattice constant a, in which each bond is present with a probability p [10–13]. Straight lines in this lattice, which have average length $(1-p)^{-1}$, are identified as fibers with stretching stiffness k and bending stiffness κ. The lattice sites are freely rotating cross links. The Hamiltonian is

$$E = \frac{k}{2a}\sum_{\langle ij\rangle} g_{ij}(|\mathbf{R}_{ij}| - a)^2 + \frac{\kappa}{2a}\sum_{\langle ijk\rangle} g_{ij}g_{jk}\Delta\theta_{ijk}^2, \tag{6}$$

where $g_{ij} = 1$ for bonds that are present, and zero for removed ones. The first term is the stretching energy; $|\mathbf{R}_{ij}|$ is the distance between sites i and j in the deformed state. The second term is bending; $\langle ijk\rangle$ labels three consecutive sites along a straight line in the reference state, and $\Delta\theta_{ijk}$ the change of angle determined by them.

The linear elasticity of this model is largely controlled by the central force isostatic point at $p_c \simeq 2/3$. For $p > p_c$ the deformations are mostly affine; below p_c disorder induced by the removal of bonds leads to nonaffine response. This is because the bending stiffness of the fibers is much smaller than the stretching stiffness: $\kappa/(ka^2) \ll 1$. When $\kappa = 0$, the system is a central-force lattice, with a rigidity percolation transition at p_c. The network with weak bending can be viewed as central-force network with a relevant perturbation of bending stiffness. The elasticity of such networks can be thought of as a crossover at the central-force isostatic point [11].

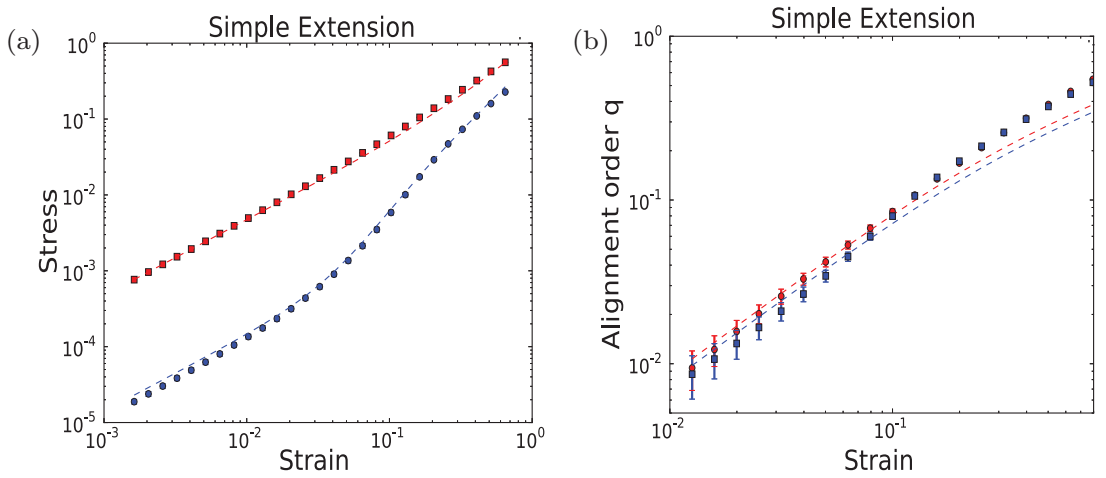

FIG. 3. (Color online) Simulation results (data points) and theory prediction (dashed lines) for simple extension at $p = 0.6$ (lower blue), and $p = 0.8$ (higher red) and $\kappa/(ka^2) = 10^{-3}$ using parameters fitted from shear and the hydrostatic expansion.

We studied this model in the nonlinear regime using 128×128 lattices. We applied three types of homogeneous deformations: simple shear, hydrostatic expansion, and simple extension. We found the stress and q as functions of strain, γ, at various values of p and $\kappa/(ka^2)$. The stress is expressed in unit of k and we take the value of the relative bending stiffness $\kappa/(ka^2)$ to be varying from 10^{-4} to 10^{-2}. This is consistent with this parameter of real collagen fibers, because the ratio $\kappa/(ka^2)$ is of the order of $(d/a)^2$, where d and a are the diameter and mesh size of the fibers, modeling the fibers as simple elastic rods.

For shear, some results are shown in Fig. 2. In agreement with our theory, the nematic order tensor $\mathbf{Q}$ does have the form $\eta(\gamma)\tilde{\mathbf{v}}$, where $\eta(\gamma)$ is a scalar. Thus the orientation of the nematic order is determined. The strength of the alignment, $q = \langle \cos 2\theta \rangle$, is a nontrivial function of γ. For small strain, the alignment is less than the purely geometric effect which occurs for affine deformations because of bending; see the Appendix. The strain at which q falls below a linear dependence on γ is hard to see in Fig. 2(b), but it is not inconsistent with the onset of nonlinearity in Fig. 2(a). For very large γ, $q \to 1$, but this is beyond the range of validity of our theory.

These results are consistent our picture. Shear stiffening is strong for $p \ll p_c$ and vanishes for $p > p_c$. The characteristic strain, γ^*, where the strain stiffening takes place is large at small p and vanishes near p_c. These observations are consistent with the exhaustion of bending modes as the network enters the stretching dominated regime. They are related to stiffening in jammed packings [17], where scaling $\gamma^* \sim |p - p_c|$ occurs.

To make the comparison with our lattice simulation quantitative, we use Eqs. (3) and (5) in two dimensions, and expand the potential V, up to fourth order in $\mathbf{Q}$:

$$V(\mathbf{Q}) = (A/2)\mathrm{Tr}\,\mathbf{Q}^2 + (C/4!)\mathrm{Tr}\,\mathbf{Q}^4. \tag{7}$$

The odd terms vanish by symmetry in two dimensions. Since we are using an expansion of this type, we should not expect the scheme to work deep in the nonlinear regime; we expect quantitative results for relatively small q. The parameters in the theory are $\{\bar{K}, \bar{\mu}, g, t, A, C\}$.

Consider the linear regime, which is characterized by three independent slopes for stress-strain curves in simple shear and in hydrostatic expansion, and the nematic-strain curve in simple shear; the corresponding slopes are the shear modulus, $\mu = \bar{\mu} - t^2/(2A)$, the bulk modulus, $K = \bar{K} - 2g/A$, and t/A. By symmetry, there cannot be any average induced nematic order in the hydrostatic expansion case, and this is what we find in simulation. The rest of the parameters are obtained in the nonlinear regime. We fit them using simulation for hydrostatic expansion for g and simple shear for the rest, separately via least-square fitting. The details of the computation are given in the Appendix. The results are shown in Fig. 2.

Strain-stiffening depends strongly on p. This is captured by the parameter C, which controls where the potential becomes strongly nonlinear and increases μ. Consider $C(p)$, Fig. 2(c): there is a sharp peak at p_c, showing that γ^* vanishes as $p \to p_c^-$. Also, consider the strain-alignment curve. Its slope is t/A for small strain. When $p \to 1$ the deformations are affine; the alignment is a geometric quantity so that $t/A \to$ a constant. This is consistent with our fitting results. However, above p_c we expect little renormalization of μ, so that t^2/A is small. We conclude, and we do find that both t and A go to zero above p_c in such a way that their ratio is constant.

We used the fitted parameters to calculate the stress-strain and nematic-strain curves for simple extension. In Fig. 3 we compare to simulation. The agreement is fairly good, except for q at large alignments which is beyond the range of validity of our theory.

IV. LOCALIZED PERTURBATION: A CONTRACTING CELL IN A MEDIUM

We now put a "cell" in the ECM by cutting a circular hole in the material and applying a negative pressure to the exposed surface to represent the contractile force of the cell [4,18]. This is done in Landau theory by applying boundary conditions. For the lattice model, we apply forces to nodes of the lattice at radius of several lattice spacings and relax the lattice. A real cell is more like a force dipole, and we could use an elliptical hole to represent this. We start with the simplest case.

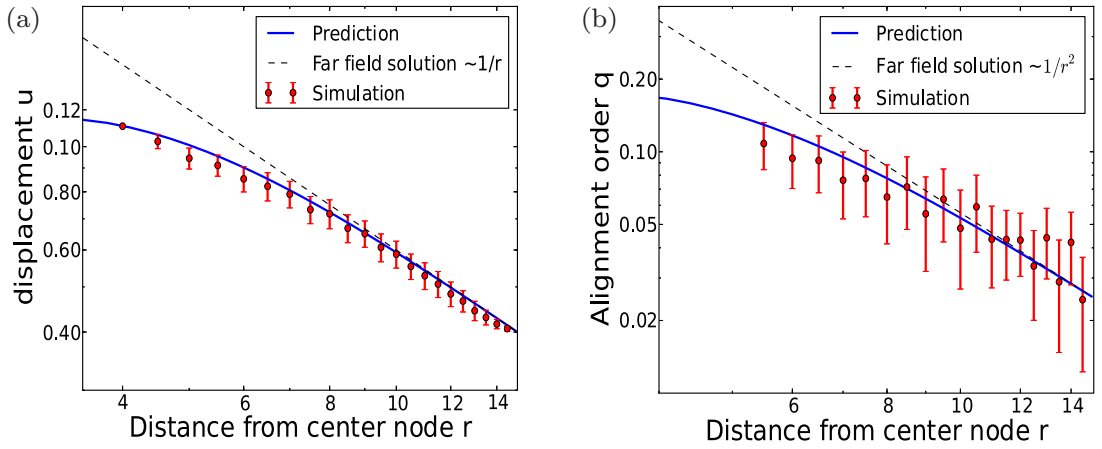

FIG. 4. (Color online) Simulation results (points) and theory predictions (solid lines) for a model for a cell in ECM using the parameters from the homogeneous deformation case.

To use Eq. (3) in this case, we note that we have two variables which depend on the distance, r, from the center of the hole: they are the radial component of the displacement, $u(r)$, and the radial alignment, $q(r)$. If we minimize F with respect to u,q we find

$$u''(r)+\frac{u'(r)}{r}-\frac{u(r)}{r^2}=\frac{t}{K+\bar{\mu}}\left(\frac{q'(r)}{2}+\frac{q(r)}{r}\right), \quad (8)$$

$$\frac{t}{2}\left(u'(r)-\frac{u(r)}{r}\right)=V'(q). \quad (9)$$

For large r the deformation is small, and the system is linear. If we use $V\approx Aq^2/2$ we get the familiar result for deformation in two dimensions [19] $u(r)\sim 1/r$. Equation (9) implies $q\sim 1/r^2$. As r decreases we enter the nonlinear regime. Thus there is a radius within which nonlinear effects and alignment are important [4].

Alignment localization of this type is captured by our theory. For small r, q is large and the nonlinear potential leads to a weak dependence of $q(r)$ on r; that is, alignment is more or less constant near the cell [4]. We calculated $u(r)$,$q(r)$ by numerically solving Eq. (8); see Fig. 4. We did a simulation in the lattice by choosing a node and pulling in on nodes a few lattice spacings away. The two kinds of results agree, as shown in Fig. 4. This calculation applies equally to the case of a tumor spheroid in the ECM [20]. The same problem has been studied with a different elastic model in Ref. [18], and a change of sign in strain has been reported. We do not find this in our simulation or our model.

V. CONCLUSION

Now we return to contact guidance which is experimentally studied [5,6] but not well understood. Our methods give us a natural framework for modeling this effect. Suppose we have a cell moving randomly with an effective diffusion coefficient, $D_\circ$, if there is no alignment. Based on symmetry, the simplest expression for the effect of alignment is $\mathbf{D}=D_\circ(1+\alpha\mathbf{Q})$, where α is a coefficient which could be measured. Experimental studies on three-dimensional cell migration showed interesting deviations from random walk behavior, especially anisotropy [21], and our model may provide a theoretical framework to understand such phenomena.

We have given a Landau theory for elastic nonlinearity in biopolymer gels. The key idea is the introduction of $\mathbf{Q}$ as a part of the order parameter to measure the exhaustion of the bending modes. Of course, this calculation is only the beginning of a treatment for cells. In further study we will represent the cell as a force dipole rather than a spherical hole. And we will put more than one cell in the system to see the interactions.

ACKNOWLEDGMENTS

We would like to thank F. MacKintosh, C. Broedersz, M. Das, and E. Ben-Jacob for useful conversations. J.-C.F. is supported by the National Science Foundation Center for Theoretical Biological Physics (Grant No. PHY-1308264). H.L. is supported in part by the Cancer Prevention and Research Institute of Texas (CPRIT) Scholar Program of the State of Texas at Rice University.

APPENDIX A: DETAILS IN FORMULATING LANDAU-TYPE THEORY

We model the nonlinear elastic energy of biopolymer gels with the following effective free energy:

$$F=\int[2K(\sqrt{\mathrm{Det}\mathbf{\Lambda}}-1)^2+\bar{\mu}\,\mathrm{Tr}\,\tilde{\mathbf{v}}^2-t\,\mathrm{Tr}(\tilde{\mathbf{v}}\cdot\mathbf{Q})$$
$$-2(\sqrt{\mathrm{Det}\mathbf{\Lambda}}-1)\mathrm{Tr}(\mathbf{h}\cdot\mathbf{Q})+V(\mathbf{Q})]d^2r,$$

where K,$\bar{\mu}$ are the bulk and shear modulus, respectively, and $\tilde{\mathbf{v}}$ is the traceless part of (left) Cauchy-Green strain tensor. It has the following definition:

$$\mathbf{v}=\frac{1}{2}(\mathbf{\Lambda}\mathbf{\Lambda}^T-\mathbf{I}),$$
$$\tilde{\mathbf{v}}=\mathbf{v}-dimension^{-1}\cdot(\mathrm{Tr}\,\mathbf{v})\mathbf{I}, \quad (A1)$$

where $\Lambda_{ij}=\frac{\partial R_i}{\partial r_j}$. $\mathbf{R}(\mathbf{r})$ is the position after(before) deformation. Under this definition, the strain tensor depends on the displacement field $\mathbf{u}(\mathbf{r})$:

$$v_{ij}\equiv(\partial_i u_j+\partial_j u_i+\partial_l u_j\partial_l u_j)/2. \quad (A2)$$

In our free-energy expression, we substitute the term Tr$\mathbf{v}$ with $2(\sqrt{\text{Det}\mathbf{\Lambda}}-1)$ to avoid redundant nonlinearity in Tr$\mathbf{v}$ under large deformation. As we will see, these two terms are equal for small deformation.

The first term in our free-energy expression is the energy caused by the change of volume. The second term is the energy contributed by the change of shape. The third shows coupling between strain and alignment. The fourth term tells a fixed random field $\mathbf{h}$ guides the alignment. The last one is the alignment energy.

1. Hydrostatic deformation

For hydrostatic deformation, it satisfies

$$\mathbf{\Lambda}=\begin{pmatrix}1+\gamma & 0\\ 0 & 1+\gamma\end{pmatrix}. \tag{A3}$$

[We can easily test that $\text{Tr}\mathbf{v}=2(\sqrt{\text{Det}\mathbf{\Lambda}}-1)=2\gamma$, for small γ.] Suppose (ignoring higher-order terms)

$$V(\mathbf{Q})=\frac{A}{2}\text{Tr}\mathbf{Q}^2+\frac{C}{4!}\text{Tr}\mathbf{Q}^4. \tag{A4}$$

From symmetry, we know the average $\mathbf{Q}$ is a zero matrix. So in this case, only the fluctuation of $\mathbf{Q}$ will contribute to free energy. When the system gets to equilibrium:

$$\frac{\partial F}{\partial \mathbf{Q}_{ij}(\mathbf{r})}=-2(\sqrt{\text{Det}\mathbf{\Lambda}}-1)\mathbf{h}_{ij}(\mathbf{r})+A\mathbf{Q}_{ij}(\mathbf{r}) +\frac{C}{6}\mathbf{Q}_{ik}(\mathbf{r})\mathbf{Q}_{kl}(\mathbf{r})\mathbf{Q}_{lj}(\mathbf{r})=0, \tag{A5}$$

2D traceless tensors have the following property:

$$\mathbf{Q}_{ik}(\mathbf{r})\mathbf{Q}_{kl}(\mathbf{r})=-(\text{Det}\mathbf{Q})\delta_{il}. \tag{A6}$$

Thus we can rewrite Eq. (A5) as

$$-2(\sqrt{\text{Det}\mathbf{\Lambda}}-1)\mathbf{h}_{ij}+A\mathbf{Q}_{ij}-\frac{C}{6}(\text{Det}\mathbf{Q})\mathbf{Q}_{ij}=0. \tag{A7}$$

Therefore, one must have $\mathbf{Q}_{ij}(\mathbf{r})=b\cdot\mathbf{h}_{ij}(\mathbf{r})$, based on the structure of Eq. (A7). We further assume that $\mathbf{h}$ has the following form:

$$\mathbf{h}(\mathbf{r})=\eta(\mathbf{r})\big(\hat{\mathbf{m}}(\mathbf{r})\hat{\mathbf{m}}(\mathbf{r})-\tfrac{1}{2}\mathbf{I}\big), \tag{A8}$$

where η is magnitude and $\hat{\mathbf{m}}$ is a unit vector indicating locally easy direction to align. This gives statistics of $\mathbf{h}$ (assuming $\hat{\mathbf{m}}$ has random direction)

$$\langle\mathbf{h}(\mathbf{r})\rangle=0,\qquad \langle\mathbf{h}_{ij}(\mathbf{r})\mathbf{h}_{jk}(\mathbf{r}')\rangle=\frac{\eta(\mathbf{r})^2}{4}\delta(\mathbf{r}-\mathbf{r}')\delta_{ik}. \tag{A9}$$

Let $g=\frac{\eta(\mathbf{r})^2}{4}$. Then $\text{Det}\mathbf{Q}=b^2\eta(\mathbf{r})^2\text{Det}[\hat{\mathbf{m}}(\mathbf{r})\hat{\mathbf{m}}(\mathbf{r})-\frac{1}{2}\mathbf{I}]=-\frac{1}{4}b^2\eta(\mathbf{r})^2=-b^2g$. Equation (A7) simplifies to

$$0=\Big(-2(\sqrt{\text{Det}\mathbf{\Lambda}}-1)+Ab+\frac{C}{6}gb^3\Big)\mathbf{h}_{ij}$$

$$\therefore\quad 0=\Big(-2(\sqrt{\text{Det}\mathbf{\Lambda}}-1)+Ab+\frac{C}{6}gb^3\Big). \tag{A10}$$

This is a scalar equation, which is independent of the direction $\hat{\mathbf{m}}$. We can get the value of b, given a fixed deformation γ, by solving Eq. (A10). Use solution b in $\mathbf{Q}_{ij}(\mathbf{r})=b\cdot\mathbf{h}_{ij}(\mathbf{r})$ and plug into F ($\tilde{\mathbf{v}}$ is zero, for hydrostatic case):

$$\begin{aligned}F&=\int[2K(\sqrt{\text{Det}\mathbf{\Lambda}}-1)^2-2(\sqrt{\text{Det}\mathbf{\Lambda}}-1)\text{Tr}(\mathbf{h}\cdot\mathbf{Q})+V(\mathbf{Q})\Big]d^2r,\\ &=\int\Big[2K(\sqrt{\text{Det}\mathbf{\Lambda}}-1)^2-2(\sqrt{\text{Det}\mathbf{\Lambda}}-1)\text{Tr}(\mathbf{h}\cdot\mathbf{Q})+\frac{A}{2}\text{Tr}\,\mathbf{Q}^2+\frac{C}{4!}\text{Tr}\,\mathbf{Q}^4\Big]d^2r,\\ &=\int\Big[2K(\sqrt{\text{Det}\mathbf{\Lambda}}-1)^2-2(\sqrt{\text{Det}\mathbf{\Lambda}}-1)b\text{Tr}\mathbf{h}^2+\frac{Ab^2}{2}\text{Tr}\mathbf{h}^2+\frac{Cb^4}{4!}\text{Tr}\mathbf{h}^4\Big]d^2r.\end{aligned} \tag{A11}$$

By taking an average, $\text{Tr}\mathbf{h}^2=2g$, $\text{Tr}\mathbf{h}^4=2g^2$. Therefore,

$$F=\int\Big[2K(\sqrt{\text{Det}\mathbf{\Lambda}}-1)^2-4gb(\sqrt{\text{Det}\mathbf{\Lambda}}-1)+Agb^2+\frac{Cg^2}{12}b^4\Big]d^2r. \tag{A12}$$

This is the elastic energy of hydrostatic deformation. In small deformation limit, we can further ignore $\frac{C}{4!}\text{Tr}\,\mathbf{Q}^4$ in free-energy expression. Then Eq. (A10) tells $b=\frac{2(\sqrt{\text{Det}\mathbf{\Lambda}}-1)}{A}$ and free-energy density $f=2K(\sqrt{\text{Det}\mathbf{\Lambda}}-1)^2-4\frac{g}{A}(\sqrt{\text{Det}\mathbf{\Lambda}}-1)^2=(2K-4\frac{g}{A})\gamma^2$. The initial slope of stress-strain curve $Slope_{\text{initial}}=\frac{\partial^2 f}{\partial\gamma^2}=4(K-2\frac{g}{A})$, which tells the random field could cause a shift in the initial slope of stress-strain curve.

2. Pure shear

For pure shear, it satisfies

$$\mathbf{\Lambda}=\begin{pmatrix}1 & \gamma\\ 0 & 1\end{pmatrix},\quad \mathbf{Q}=\begin{pmatrix}q_a & q_b\\ q_b & -q_a\end{pmatrix}. \tag{A13}$$

Let $\frac{\partial F}{\partial q_a}=0$ and $\frac{\partial F}{\partial q_b}=0$, and plugging the value of q_a,q_b back into F, we can get the free energy for the pure shear case. In particular, we can get

$$\eta_{q_a}=0,\quad \eta_{q_b}=\frac{t}{2A},\qquad \eta_q=2\eta_{q_b}=\frac{t}{A},\qquad \eta_\sigma=\tilde{\mu}-\frac{t^2}{2A}, \tag{A14}$$

where η_{q_a}, η_{q_b}, η_q, and η_σ are the initial slope of q_a-strain, q_b-strain, q-strain, and stress-strain curves, respectively.

3. Simple extension

For simple extension, it satisfies

$$\mathbf{\Lambda}=\begin{pmatrix}1+\gamma_x & 0\\ 0 & 1+\gamma_y\end{pmatrix},\quad \mathbf{Q}=\begin{pmatrix}\frac{1}{2}q & 0\\ 0 & -\frac{1}{2}q\end{pmatrix}. \tag{A15}$$

The simple extension case is more complicated, since both the shape and the volume (area for 2D case) are changed during the process. Here we apply a method similar to that for hydrostatic deformation to solve this problem. Note the method here is applicable to any kind of deformation. We start from free-energy density:

$$f = 2K(\sqrt{\mathrm{Det}\mathbf{\Lambda}} - 1)^2 + \bar{\mu}\,\mathrm{Tr}\,\tilde{\mathbf{v}}^2 - t\,\mathrm{Tr}(\tilde{\mathbf{v}}\cdot\mathbf{Q}) - 2(\sqrt{\mathrm{Det}\mathbf{\Lambda}} - 1)\mathrm{Tr}(\mathbf{h}\cdot\mathbf{Q}) + \frac{A}{2}\mathrm{Tr}\,\mathbf{Q}^2 + \frac{C}{4!}\mathrm{Tr}\,\mathbf{Q}^4.$$

For convenience we introduce the notation

$$Y = 2(\sqrt{\mathrm{Det}\mathbf{\Lambda}} - 1). \tag{A16}$$

We can easily test that $Y = \mathrm{Tr}\mathbf{v}$ for small γ. The equation for variation of $\mathbf{Q}$ (it contains two parts, nonzero expectation and fluctuation, but it's still traceless) is

$$\frac{\partial F}{\partial \mathbf{Q}_{ij}(\mathbf{r})} = -Y\mathbf{h}_{ij} - t\tilde{\mathbf{v}}_{ij} + A\mathbf{Q}_{ij}(\mathbf{r}) + \frac{C}{6}\mathbf{Q}_{ik}\mathbf{Q}_{kl}\mathbf{Q}_{lj} = 0. \tag{A17}$$

Repeating what we did in the hydrostatic case and letting $\mathbf{M} = -Y\mathbf{h} - t\tilde{\mathbf{v}}$, we have

$$\mathbf{M} + A\mathbf{Q} - \frac{C}{6}(\mathrm{Det}\mathbf{Q})\mathbf{Q} = 0. \tag{A18}$$

Take ansatz $\mathbf{Q} = \alpha\mathbf{M}$, where α is a scalar and then cancel M,

$$1 + A\alpha - \frac{C}{6}\alpha^3(\mathrm{Det}\mathbf{M}) = 0. \tag{A19}$$

By solving Eq. (A19) we know the value of α. Plugging α into the free-energy expression, we can get the free energy in the end. This procedure is exactly the same as in the hydrostatic case, although the calculation is more complicated. In particular, we can get

$$\eta_q = \frac{4K't}{2A(K' + \tilde{\mu}) - t^2},$$
$$\eta_\sigma = \frac{4K'(2\tilde{\mu}A - t^2)}{2A(K' + \tilde{\mu}) - t^2}, \tag{A20}$$
$$\text{where}\quad K' = K - \frac{2g}{A}.$$

Not surprisingly, the initial slopes of the pure extension case can be expressed as a function of initial slopes of the pure shear case and hydrostatic case:

$$\eta_{q,\mathrm{extension}} = \frac{4\eta_{\sigma,\mathrm{hydro}}\eta_{q_b,\mathrm{shear}}}{\eta_{\sigma,\mathrm{hydro}} + 4\eta_{\sigma,\mathrm{shear}}},$$
$$\eta_{\sigma,\mathrm{extension}} = \frac{4\eta_{\sigma,\mathrm{hydro}}\eta_{\sigma,\mathrm{shear}}}{\eta_{\sigma,\mathrm{hydro}} + 4\eta_{\sigma,\mathrm{shear}}}. \tag{A21}$$

Equation (A21) is a simple way to test the correctness of our theory. The second equation here can also be derived from the free-energy expression in Landau's book, which is to say that our theory is consistent with Landau's in the small deformation limit.

4. Circular symmetry case

From homogenous deformation, we can see the nonlinearity in the shearing case attributes to the expectation of alignment $\mathbf{Q}$, while in the hydrostatic extension case attributes to the fluctuation of alignment $\mathbf{Q}$. Generally speaking, both the expectation and variation of $\mathbf{Q}$ play roles in stiffening for an arbitrary deformation mode. However, in the circular symmetry case we study here, the expectation of $\mathbf{Q}$ is more important. We can see that from a slightly different free-energy expression form:

$$F = \int [2K(\sqrt{\mathrm{Det}\mathbf{\Lambda}} - 1)^2 + \bar{\mu}\,\mathrm{Tr}\,\tilde{\mathbf{v}}^2 - t\,\mathrm{Tr}(\tilde{\mathbf{v}}\cdot\mathbf{Q}) + K_{\mathrm{nonlinear}}(\sqrt{\mathrm{Det}\mathbf{\Lambda}} - 1)^3 + V(\mathbf{Q})]d^2r.$$

In this free-energy expression, we substitute $-2(\sqrt{\mathrm{Det}\mathbf{\Lambda}} - 1)\mathrm{Tr}(\mathbf{h}\cdot\mathbf{Q})$ with $K_{\mathrm{nonlinear}}(\sqrt{\mathrm{Det}\mathbf{\Lambda}} - 1)^3$. Now we only consider the expectation of $\mathbf{Q}$ and the new term explains the nonlinearity in hydrostatic extension. By solving the equilibrium equation of the system, we find the value of $K_{\mathrm{nonlinear}}$ has little influence on the solution (for network with bending stiffness $\frac{\kappa}{ka^2} = 10^{-3}$). That is to say the nonlinearity in $u - r$ and $q - r$ curves are mainly caused by the change of shape in this case.

As we have mentioned above, in linear regime of hydrostatic deformation, $f = 2K(\sqrt{\mathrm{Det}\mathbf{\Lambda}} - 1)^2 - 4\frac{g}{A}(\sqrt{\mathrm{Det}\mathbf{\Lambda}} - 1)^2 = (2K - 4\frac{g}{A})\gamma^2 = (\frac{K}{2} - \frac{g}{A})\mathrm{Tr}\mathbf{v}^2 = \frac{K'}{2}\mathrm{Tr}\mathbf{v}^2$, where $K' = K - \frac{2g}{A}$. Since the nonlinearity caused by the change of area does not matter much in this problem, we can use this linear approximation to simplify the free-energy expression:

$$f = \tilde{\mu}\tilde{v_{ij}}^2 + \tfrac{1}{2}K'(v_{ii})^2 - t\tilde{v_{ij}}Q_{ij} + V(q), \tag{A22}$$

Now the only effect of random field is a shift in the bulk modulus. By definition, $\mathbf{Q} = q(\hat{\mathbf{n}}\hat{\mathbf{n}} - \frac{1}{2}\mathbf{I})$, where $\mathbf{n}$ is the director of nematic order tensor $\mathbf{Q}$. Then we can calculate the differential of free-energy density:

$$df = [K'\delta_{ij}v_{ll} + (2\tilde{\mu}\tilde{v_{ij}} - tQ_{ij})]dv_{ij} + \left[-t\tilde{v}_{ij}\left(\hat{n}_i\hat{n}_j - \frac{1}{2}\delta_{ij}\right) + V'(q)\right]dq. \tag{A23}$$

Now we have the relation between strain $\mathbf{v}$ and stress $\boldsymbol{\sigma}$:

$$\sigma_{ij} = K'\delta_{ij}v_{ll} + (2\tilde{\mu}\tilde{v_{ij}} - tQ_{ij}). \tag{A24}$$

In linear elasticity, $\mathbf{v} = \mathbf{u}$, we can write

$$\sigma_{ij} = K'\delta_{ij}v_{ll} + 2\tilde{\mu}v_{ij} - \tilde{\mu}v_{ll}\delta_{ij} - tQ_{ij} = (K' - \tilde{\mu})v_{ll}\delta_{ij} + 2\tilde{\mu}v_{ij} - tQ_{ij}. \tag{A25}$$

By force equilibrium, $\partial_j\sigma_{ij} = 0$,

$$(K' - \tilde{\mu})\partial_i\partial_l u_l + \tilde{\mu}(\partial_j^2 u_i + \partial_j\partial_i u_j) - t\partial_j Q_{ij} = 0. \tag{A26}$$

We can rewrite it in the following form:

$$[K' \bigtriangledown (\bigtriangledown\cdot\mathbf{u}) + \tilde{\mu}\bigtriangleup\mathbf{u}]_i - t\partial_j Q_{ij} = 0. \tag{A27}$$

Using $\bigtriangledown(\bigtriangledown\cdot\mathbf{u}) = \bigtriangleup\mathbf{u}$ in the 2D case,

$$[(K' + \tilde{\mu})\bigtriangleup\mathbf{u}]_i - t\partial_j Q_{ij} = 0. \tag{A28}$$

For the circular symmetry case, it satisfies

$$\mathbf{u} = u(r)\hat{\mathbf{r}},$$
$$Q_{ij} = q(r)\left(\hat{\mathbf{r}}\hat{\mathbf{r}} - \frac{1}{2}\mathbf{I}\right). \tag{A29}$$

Plug Eq. (A29) into $\partial_j Q_{ij}$; after some simplification, we have

$$\partial_j Q_{ij} = \hat{r}_i \left(\frac{q'(r)}{2} + \frac{q(r)}{r} \right). \tag{A30}$$

Plugging Eq. (A30) into Eq. (A28), we finally have

$$u''(r) + \frac{u'(r)}{r} - \frac{u(r)}{r^2} = \frac{t}{K' + \tilde{\mu}} \left(\frac{q'(r)}{2} + \frac{q(r)}{r} \right). \tag{A31}$$

When free energy is minimized, $\frac{\partial F}{\partial q} = 0$, according to Eq. (A23),

$$\begin{aligned} -t\tilde{v}_{ij} \left(\hat{r}_i \hat{r}_j - \frac{1}{2}\delta_{ij} \right) + V'(q) = 0, \\ \therefore -t \left(v_{rr} - \frac{1}{2}\mathrm{Tr}\mathbf{v} \right) + V'(q) = 0. \end{aligned} \tag{A32}$$

Using the fact that $v_{rr} = u'(r), \mathrm{Tr}(\mathbf{v}) = u(r) + \frac{u'(r)}{r}$, here is the final form:

$$\frac{t}{2} \left(u'(r) - \frac{u(r)}{r} \right) = V'(q). \tag{A33}$$

Here $V(q) = \frac{A}{2}\mathrm{Tr}(\mathbf{Q}^2) + \frac{C}{4!}\mathrm{Tr}(\mathbf{Q}^4)$.

Now we have two coupled equations: Eq. (A31) and Eq. (A33). By solving them, we can get the numerical solution of the system.

In far field, q value is small enough that we only keep the leading term in $V(q)$:

$$V(q) = \frac{A}{2}\mathrm{Tr}(\mathbf{Q}^2) = \frac{A}{4}q^2. \tag{A34}$$

Also, we can drop the nonlinear term $g\,\mathrm{Tr}(\mathbf{v})^3$ since the nonlinearity is weak in far field. Under these conditions, we get solution

$$u(r) \sim \frac{1}{r}, \quad q(r) \sim \frac{1}{r^2}. \tag{A35}$$

APPENDIX B: SIMULATION

1. Homogeneous case

We studied this lattice numerically in the nonlinear regime using 128×128 triangular lattices. Three different types of homogeneous deformations are applied here: Pure shear, hydrostatic extension, and simple extension. For hydrostatic extension, we apply fixed boundary condition, while periodic boundary condition is applied for pure shear and simple extension. For each γ, we deform the network according to its value and deformation mode, then relax the internal degrees of freedom by minimizing the energy using a conjugate-gradient algorithm. By varying the value of γ, the stress and nematic order as functions of γ are obtained.

For all figures in our paper, $\frac{\kappa}{ka^2} = 10^{-3}$. (We also explore $\frac{\kappa}{ka^2}$ from 10^{-1}–10^{-4}, which generates similar results.) The value of γ is the range of $[0.001, 1]$.

The value of parameters in our model are obtained in the following procedure.

(1) The initial slope of stress-strain curve of hydrostatic extension is $4(K - 2\frac{g}{A})$.

(2) From Eq. (A14), we can know the value of $\frac{t}{A}$ and $\tilde{\mu} - \frac{t^2}{2A}$ from the initial slope of q-strain and stress-strain curve under pure shear. (Actually we get the value of $\frac{t}{2A}$ from q_b-strain curve to reduce the effect of residue alignment.)

(3) The value of K and μ can be decided in the following way.

(i) For a network with the same parameters except the probability of bond existence $p = 1$, stress-strain and q-strain curves are purely linear. The initial slope of stress-strain curve of hydrostatic extension for this network is $4K_{100}$. The initial slope of stress-strain curve of shearing is μ_{100}.

(ii) μ, K satisfy $\mu = p \cdot \mu_{100}$ and $K = p \cdot K_{100}$. For example, if $p = 0.6$, then $\mu = 0.6 \cdot \mu_{100}$.

(4) Now all parameters except C have been determined. We decide the value of C by minimizing the error between simulation result and our theory. [Three curves are involved: stress strain (hydrostatic), stress strain (shearing), and q strain (shearing).]

After all parameter values are collected in our model, a prediction for simple extension can be made.

2. Circular symmetry case

For the circular symmetry case, $p = 0.6$ and $\frac{\kappa}{ka^2} = 10^{-3}$. The value of parameters are first collected by fitting the network with the same p, κ value under homogeneous deformation. To simulate the circular symmetry case, a central node in the network is picked and nodes are pulled at the distance at $r = 4$ bond length (inner boundary) and at $r = 15$ bond length (outer boundary) towards the central node. Then the nodes on the boundary are fixed and internal degree of freedom are relaxed by minimizing free energy. $u(r)$ and $q(r)$ are calculated by taking the average value within a ring, which is r bond length away from the center. In the end, we set the boundary condition of Eq. (A31) and Eq. (A33) with the displacement of nodes on the boundaries in simulation and plug in the parameter value. By solving these two nonlinear equations, our model provides a prediction for simulation.

3. Alignment in affine vs nonaffine deformations

In this paper we defined the alignment order parameter Q using the actual deformation of the lattice sites, which

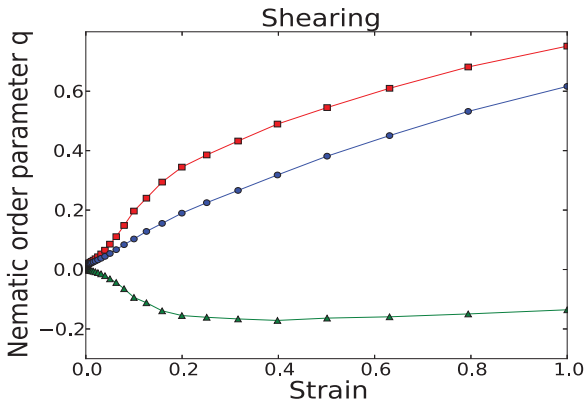

FIG. 5. (Color online) Comparison of q_{affine} (top red), q (middle blue), and $q - q_{\mathrm{affine}}$ (bottom green) for a simple extension at $p = 0.6$ and $\kappa/(ka^2) = 10^{-3}$.

is necessarily nonaffine due to the disordered structure of the lattice. In an affine deformation (same deformation everywhere; usually not the lowest-energy configuration in disordered systems) the fibers also become aligned, and this alignment, which we call Q_{affine}, is a pure *geometrical quantity* and can be easily calculated. The full alignment Q can be either greater or smaller than Q_{affine}, depending on the deformation. In Fig. 5 we show one example of such a comparison.

[1] N. Wang and D. E. Ingber, Biochem. Cell Biol. **73**, 327 (1995).
[2] M. Gardel, J. Shin, F. MacKintosh, L. Mahadevan, P. Matsudaira, and D. Weitz, Science **304**, 1301 (2004).
[3] C. Storm, J. Pastore, F. MacKintosh, T. Lubensky, and P. Janmey, Nature (London) **435**, 191 (2005).
[4] L. M. Sander, J. Biomech. Eng. **135**, 071006 (2013).
[5] P. A. Agudelo-Garcia, J. K. De Jesus, S. P. Williams, M. O. Nowicki, E. A. Chiocca, S. Liyanarachchi, P.-K. Li, J. J. Lannutti, J. K. Johnson, and S. E. Lawler, Neoplasia (New York, NY) **13**, 831 (2011).
[6] D. Vader, A. Kabla, D. Weitz, and L. Mahadevan, PLoS ONE **4**, e5902 (2009).
[7] A. M. Stein, D. A. Vader, D. A. Weitz, and L. M. Sander, Complexity **16**, 22 (2011).
[8] P. R. Onck, T. Koeman, T. van Dillen, and E. van der Giessen, Phys. Rev. Lett. **95**, 178102 (2005).
[9] T. C. Lubensky, R. Mukhopadhyay, L. Radzihovsky, and X. Xing, Phys. Rev. E **66**, 011702 (2002).
[10] M. Das, F. C. MacKintosh, and A. J. Levine, Phys. Rev. Lett. **99**, 038101 (2007).
[11] C. P. Broedersz, X. Mao, T. C. Lubensky, and F. C. MacKintosh, Nat. Phys. **7**, 983 (2011).
[12] M. Das, D. A. Quint, and J. M. Schwarz, PloS one **7**, e35939 (2012).
[13] X. Mao, O. Stenull, and T. C. Lubensky, Phys. Rev. E **87**, 042601 (2013).
[14] E. Cosserat and F. C. Cosserat, *Thorie des Corps Dformables* (Hermann et Fils, Paris, 1909).
[15] I. Kunin, *Elastic Media and Microstructure II* (Springer, Berlin, 1983).
[16] M. Sheinman, C. P. Broedersz, and F. C. MacKintosh, Phys. Rev. E **85**, 021801 (2012).
[17] M. Wyart, H. Liang, A. Kabla, and L. Mahadevan, Phys. Rev. Lett. **101**, 215501 (2008).
[18] Y. Shokef and S. A. Safran, Phys. Rev. Lett. **108**, 178103 (2012).
[19] L. D. Landau, E. M. Lifshitz, A. M. Kosevich, and L. P. Pitaevskii, *Theory of Elasticity* (Pergamon Press, Oxford, 1986).
[20] Q. Shi, R. P. Ghosh, H. Engelke, C. H. Rycroft, L. Cassereau, J. A. Sethian, V. M. Weaver, and J. T. Liphardt, Proc. Natl. Acad. Sci. U.S.A. **111**, 658 (2014).
[21] P.-H. Wu, A. Giri, S. X. Sun, and D. Wirtz, Proc. Natl. Acad. Sci. U.S.A. **111**, 3949 (2014).